

# Ab-initio wave-length dependent Raman spectra: Placzek approximation and beyond.

Michael Walter<sup>\*,†</sup> and Michael Moseler<sup>†</sup>

<sup>†</sup>*Fraunhofer IWM, MikroTribologie Centrum  $\mu TC$ , Wöhlerstrasse 11, D-79108 Freiburg, Germany*

<sup>‡</sup>*FIT Freiburg Centre for Interactive Materials and Bioinspired Technologies, Georges-Köhler-Allee 105, 79110 Freiburg, Germany*

<sup>¶</sup>*Physikalisches Institut, Universität Freiburg, Herrmann-Herder-Straße 3, D-79104 Freiburg, Germany*

<sup>§</sup>*Freiburger Materialforschungszentrum, Universität Freiburg, Stefan-Meier-Straße 21, D-79104 Freiburg, Germany*

E-mail: Michael.Walter@mf.uni-freiburg.de

June 14, 2019

## Abstract

We analyze how to obtain non-resonant and resonant Raman spectra within the Placzek as well as the Albrecht approximation. Both approximations are derived from the matrix element for light scattering by application of the Kramers, Heisenberg and Dirac formula. It is shown that the Placzek expression results from a semi-classical approximation of the combined electronic and vibrational transition energies. Molecular hydrogen, water and butadiene are studied as test cases. It turns out that the Placzek approximation agrees qualitatively with the more accurate Albrecht formulation even

in the resonant regime for the excitations of single vibrational quanta. However, multiple vibrational excitations are absent in Placzek, but can be of similar intensities as single excitations under resonance conditions. The Albrecht approximation takes multiple vibrational excitations into account and the resulting simulated spectra exhibit good agreement with experimental Raman spectra in the resonance region as well.

## 1 Introduction

Raman spectroscopy is a facile and nondestructive tool for the investigation of materials properties and is applied in various fields of materials research. The Raman effect couples light scattering to vibrational modes and thus involves both electronic and nuclear degrees of freedom as well as the coupling thereof. The complex properties of Raman spectra has entered excellent textbooks<sup>1,2</sup>.

Despite the general availability in experiment, the theoretical basis of the Raman effect is rather involved as it is a second order process in the electronic degrees of freedom that are coupled to nuclear vibrational degrees of freedom. Nevertheless, the calculation of Raman spectra by ab initio techniques has a long history. In the past, most approaches are based on the powerful Placzek approximation. In this approximation the Raman intensity is proportional to the derivatives of the polarizability tensor with respect to nuclear coordinates<sup>1,3</sup>. In chemistry related literature, the Placzek approximation is usually applied only for excitation energies far from resonance and a large fraction of approaches deduce the Raman intensities from static polarizability derivatives.<sup>3-9</sup> Some derivations go beyond this, but restrict the calculation also to a single frequency far from resonance<sup>10-13</sup>. The Placzek approximation is frequently used in the resonance region in solid state Raman spectroscopy.<sup>14-17</sup> This has been criticized by some authors.<sup>18</sup>

There are many approaches to address also resonant Raman spectra that mostly start from the assumption that only Franck-Condon-type scattering is important<sup>19-24</sup>. Apart from pioneering early calculations<sup>25</sup>, only recently the application of an alternative formulation

within the Albrecht approximation<sup>26–29</sup> has become tractable within standard electronic structure theory<sup>30–34</sup>. In these approaches often only the resonant part is taken into account<sup>31,35–37</sup> or the calculation is restricted to the static limit<sup>30</sup>.

In the present work we study the calculation of Raman spectra of small molecules in order to benchmark the different approaches used in the literature and to elucidate their connection. In particular, a formalism is presented that yields the Placzek as well as the Albrecht approximations from the Heisenberg-Kramers-Dirac matrix element. In this way the connection between the two approximations can be worked out explicitly.

This article is organized as follows. The underlying theoretical approach is detailed in the following section. Section 3 describes the computational approach and the following sections reports the differences and similarities of the different levels of theory for small molecules.

## 2 Theory

Raman scattering is nonelastic light scattering, where a system of initial energy  $E_I$  absorbs a photon of energy  $\hbar\omega_L$  with polarization  $\mathbf{u}_L$  and ends up in a state of energy  $E_F$  having emitted a photon with energy  $\hbar\omega_S$  and polarization  $\mathbf{u}_S$ . The cross section for this process can be expressed as<sup>3,23,27,31</sup>

$$\frac{d\sigma}{d\Omega} = \frac{\omega_L\omega_S^3}{(4\pi\epsilon_0)^2c^4} |V_{FI}|^2 \delta(E_I + \hbar\omega_L - E_F - \hbar\omega_S) \quad (1)$$

where the  $\delta$ -function ensures energy conservation. The second order matrix element for light scattering  $V_{FI}$  has been derived by Kramers, Heisenberg and Dirac and can be written as<sup>29,38–41</sup>

$$V_{FI} = \mathbf{u}_L \cdot \sum_{K \neq I} \left[ \frac{\langle I|\mathbf{D}|K\rangle\langle K|\mathbf{D}|F\rangle}{E_K - E_I - \hbar\omega_L} + \frac{\langle K|\mathbf{D}|F\rangle\langle I|\mathbf{D}|K\rangle}{E_K - E_I + \hbar\omega_S} \right] \cdot \mathbf{u}_S, \quad (2)$$

where  $\mathbf{D}$  denotes the dipole operator, a vector with the unit of length times charge. Initial and final states are denoted by  $|I\rangle$  and  $|F\rangle$ , respectively, and include nuclear as well as

electronic degrees of freedom. The sum extends over all intermediate states  $|K\rangle$  of the system with their energies  $E_K$ . Often an imaginary part is added to the photon energies  $\hbar\omega_L$  and  $\hbar\omega_S$  in eq. (2). This does not affect our further derivations, however.

In order to make the calculation tractable, the Born-Oppenheimer approximation has to be applied resulting in the separation of electronic and nuclear degrees of freedom. For Raman scattering, the electronic ground state is adopted both in the initial and the final states. We therefore write the initial state  $|I\rangle$  ( $I \equiv 0, i^0$ ) and final state  $|F\rangle$  ( $F \equiv 0, f^0$ ) as products of the electronic ground state  $|0\rangle$  and the corresponding initial  $|i^0\rangle$  and final  $|f^0\rangle$  vibrational states. The intermediate states  $|K\rangle$  ( $K \equiv e, k^e$ ) are products of excited electronic states  $|e\rangle$  and the corresponding vibrational states  $|k^e\rangle$ . Furthermore, we assume that the light is exclusively absorbed by the electronic system, i.e. no photon absorption by the nuclear wave function is considered. This should be a good approximation for the usual laser frequencies in the optical range utilized in Raman spectroscopy. The dipole transition matrix elements expressed in these states can be written as

$$\langle I|\mathbf{D}|K\rangle = \langle i^0|\mathbf{m}_e(\xi)|k^e\rangle, \quad \mathbf{m}_e(\xi) = \langle 0(\xi)|\mathbf{D}|e(\xi)\rangle, \quad (3)$$

where the dependence of the electronic states on the nuclear coordinates  $\xi$  is made explicit. Using the electronic energies of ground and excited states  $E_0$  and  $E_e$ , and the corresponding vibrational energies  $\varepsilon_k^e$  and  $\varepsilon_i^0$ , we may express the matrix element as

$$V_{FI} = \mathbf{u}_L \cdot \sum_e \sum_k \left[ \frac{\langle i^0|\mathbf{m}_e|k^e\rangle\langle k^e|\mathbf{m}_e^*|f^0\rangle}{E_e - E_0 + \varepsilon_k^e - \varepsilon_i^0 - \hbar\omega_L} + \frac{\langle k^e|\mathbf{m}_e^*|f^0\rangle\langle i^0|\mathbf{m}_e|k^e\rangle}{E_0 - E_e + \varepsilon_k^e - \varepsilon_i^0 + \hbar\omega_S} \right] \cdot \mathbf{u}_S. \quad (4)$$

Despite that the energies  $E_0$  and  $E_e$  correspond to the electronic system they are not depending on nuclear coordinates at this point. Within the independent mode double harmonic (IMDHO)<sup>42</sup> approximation the energies represent the minima of the of the harmonic oscillators shown in Fig. 1 below.

**MW: A:** Note, that the matrix element  $V_{FI}$  itself does not select initial and final vibrational

states  $i^0$  and  $f^0$ , respectively. State selection is enforced by energy conservation in eq. (1). The energy difference between the laser and the emitted photon directly reflects the energy difference of vibrational states as

$$\hbar\omega_L - \hbar\omega_S = E_F - E_I = \varepsilon_f^0 - \varepsilon_i^0 . \quad (5)$$

This difference is positive for Stokes and negative for Anti-Stokes scattering.

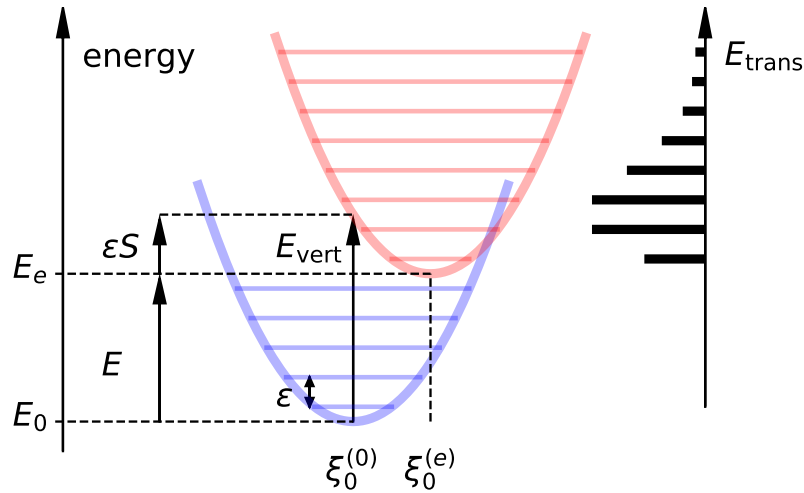


Figure 1: Displaced harmonic oscillator model for the electronic ground state (blue) and one excited state (red). The black bars on the right show the size of the squared Franck-Condon factors for a transition from the vibrational ground state.

Starting from (4) the widely used Placzek approximation is obtained by employing the semi-classical approximation<sup>43</sup> to replace the energy terms  $E_e - E_0 + \varepsilon_k^e - \varepsilon_i^0$  by their main contribution that is the vertical transition energy to this specific electronic state, i.e.

$$E_e - E_0 + \varepsilon_k^e - \varepsilon_i^0 \approx E_{\text{vert},e} , \quad (6)$$

see Fig. 1. The vertical transition energy depends on the nuclear position and is understood

to be inside of the matrix element involving the initial vibrational state  $|i^0\rangle$ . The equivalent application of a classical Wigner phase space approximation<sup>43,44</sup> leads to the same result. We will discuss the validity of this assumption further below. Applying the approximation (6) the  $k$ -dependence of the denominator in eq. (4) vanishes, and the closure relation within the vibrational subspace can be used<sup>18</sup>

$$\sum_k |k^e\rangle\langle k^e| = I_{\text{vib},e} \quad (7)$$

leading to

$$V_{FI} = \langle i^0 | \mathbf{u}_L \cdot \sum_e \left[ \frac{\mathbf{m}_e \mathbf{m}_e^*}{E_{\text{vert},e} - \hbar\omega_L} + \frac{\mathbf{m}_e^* \mathbf{m}_e}{E_{\text{vert},e} + \hbar\omega_S} \right] \cdot \mathbf{u}_S | f^0 \rangle. \quad (8)$$

In case of real valued wave functions (as can always be assumed the case of finite systems in absence of magnetic fields) and using  $\omega_L \approx \omega_S$  in the denominator, this matrix element further reduces to

$$V_{FI} = \mathbf{u}_L \cdot \langle i^0 | \alpha(\omega_L) | f^0 \rangle \cdot \mathbf{u}_S \quad (9)$$

where the polarizability tensor

$$\alpha(\omega) = \sum_e \frac{2E_{\text{vert},e} \mathbf{m}_e \mathbf{m}_e}{E_{\text{vert},e}^2 - \hbar^2 \omega^2}. \quad (10)$$

of the system in its electronic ground state emerges.

Eq. (9) has important consequences as it represents the overlap between initial and final vibronic states in the electronic ground state that are orthonormal. In order to get a non-vanishing vibrational contribution (apart from the Rayleigh scattering, where  $f^0 = i^0$ ), an operator depending on vibrational coordinates is required. This dependence can be extracted by expanding  $\alpha(\omega)$  in terms of normal vibrational coordinates<sup>3</sup>  $Q_v$  around the

nuclear equilibrium position  $\xi_0$ , where usually only the first order is taken into account

$$\alpha(\omega; \xi) = \alpha(\omega; \xi_0) + \sum_v \left. \frac{\partial \alpha(\omega; \xi_0)}{\partial Q_v} \right|_{Q_v=0} Q_v . \quad (11)$$

The first term in the expansion (11) corresponds to Rayleigh scattering and the second term contributes to the Raman effect giving

$$|V_{FI}|^2 = \sum_v |\langle i^0 | Q_v | f^0 \rangle|^2 \left| \mathbf{u}_L \cdot \frac{\partial \alpha(\omega_L)}{\partial Q_v} \cdot \mathbf{u}_S \right|^2 . \quad (12)$$

The orthogonality of the vibrational states in the electronic ground state shows that coupling to vibrational excitations is due to the first derivatives in eq. (11) only, and that only single vibrational quanta can be introduced by light scattering within this approximation. Anharmonic effects or mode mixing<sup>12,13,45</sup> might lead to multiple vibrational excitations. These effects are of second order in the derivative after vibrational coordinates (c.f. Fig. 2 below) and thus beyond the IMDHO model applied here.

The Placzek approximation is very successful for molecules. These have a large electronic “gap”, such that the usual experimental excitation wavelengths  $\omega_L$  in the infrared or visible regions are far from any electronic resonances of the molecules. Many calculations even assume the limit  $\omega_L \rightarrow 0$  and calculate  $I_{\text{Ram},v}$  from the static polarizability derived by calculations with static electric fields<sup>3,9,16,46–50</sup>. This intensity is often interpreted as “the” Raman intensity although experimental approaches report a wavelength dependence of Raman spectra since decades<sup>29</sup>.

The assumption that all electronic resonances are far from  $\hbar\omega_L$  is not valid anymore in solids. Raman spectra are the primary source of information to characterize amorphous carbon for example, where the usual  $\omega_L$  are well in the range of electronic excitation frequencies.<sup>51</sup> Therefore strong effects from variations in  $\omega_L$  are reported.<sup>52</sup> This motivated Profeta and Mauri<sup>18</sup> to express eq. (8) as function of two independent sets of nuclear coordinates

$\xi, \xi'$  in  $\mathbf{m}_e$  and  $E_{\text{vert},e}$ , respectively. The polarizability tensor reads then

$$\alpha(\omega; \xi, \xi') = \sum_e \frac{2E_{\text{vert},e}(\xi') \mathbf{m}_e(\xi) \mathbf{m}_e(\xi)}{E_{\text{vert},e}^2(\xi') - \hbar^2 \omega^2}. \quad (13)$$

The authors give some reasoning to consider the derivatives after  $\xi$  in  $\mathbf{m}_e$ , only, which obviously is only part of the contribution. We will call this contribution ‘‘Profeta’’ that is

$$|V_{FI}^{\text{Profeta}}|^2 = \sum_v |\langle i^0 | Q_v | f^0 \rangle|^2 \left| \mathbf{u}_L \cdot \frac{\partial \alpha(\omega_L; \xi, \xi')}{\partial Q_v} \cdot \mathbf{u}_S \right|^2 \quad (14)$$

with the vibrational coordinates  $Q_v$  corresponding to the nuclear coordinates  $\xi$ . This part is labeled ‘‘three-band terms’’ by Wang et al.<sup>17</sup> We name the remaining part of (8) ‘‘Pl/Pr’’ as shorthand for Placzek without Profeta in the following. It explicitly reads

$$|V_{FI}^{\text{Pl/Pr}}|^2 = \sum_v |\langle i^0 | Q_v | f^0 \rangle|^2 \left| \mathbf{u}_L \cdot \frac{\partial \alpha(\omega_L; \xi, \xi')}{\partial Q'_v} \cdot \mathbf{u}_S \right|^2 \quad (15)$$

with the vibrational coordinates  $Q'_v$  corresponding to the nuclear coordinates  $\xi'$ . This part was labeled as ‘‘two-band terms’’ in Wang et al.<sup>17</sup> We will see further below that neglecting the ‘‘Pl/Pr’’ contribution can be a severe and misleading approximation at least in molecular systems as it disregards the resonant part of the Raman contributions.

In order to go beyond the Placzek approximation, one may start from eq. (4) where we note that in contrast to  $E_{\text{vert},e} = E_{\text{vert},e}(\xi)$ , all energies are independent of nuclear coordinates. We may expand already the matrix elements in terms of normal coordinates<sup>27,31,53</sup>

$$\mathbf{m}_e(\xi) = \mathbf{m}_e(\xi_0) + \sum_v \frac{\partial \mathbf{m}_e}{\partial Q_v} \Big|_{Q_v=0} Q_v. \quad (16)$$

The first term of this expansion leads to the Albrecht A term

$$V_{FI}^A = \sum_e \sum_k \mathbf{u}_L \cdot \left[ \frac{\mathbf{m}_e \langle i^0 | k^e \rangle \langle k^e | f^0 \rangle \mathbf{m}_e}{E_e - E_0 + \varepsilon_k^e - \varepsilon_i^0 - \hbar \omega_L} + \frac{\mathbf{m}_e \langle i^0 | k^e \rangle \langle k^e | f^0 \rangle \mathbf{m}_e}{E_0 - E_e + \varepsilon_k^e - \varepsilon_i^0 + \hbar \omega_S} \right] \cdot \mathbf{u}_S \quad (17)$$



where we use the shorthand notation  $\mathbf{m}_e = \mathbf{m}_e(\xi_0)$ . It is also called the Franck-Condon term<sup>31,54</sup> and is believed to be dominating for  $\omega_L$  in resonance with optically strong transitions<sup>23</sup>. Note, that a non-negligible contribution from Albrecht A to the off resonant Raman spectrum of water was reported recently.<sup>30</sup> Close to resonance often only the first part inside of the brackets is kept since this is the dominating contribution due to the small denominator. The other part is non-resonant and hence much smaller, such that

$$V_{FI}^A = \sum_e \mathbf{u}_L \cdot \mathbf{m}_e \mathbf{m}_e \cdot \mathbf{u}_S \sum_k \frac{\langle i^0 | k^e \rangle \langle k^e | f^0 \rangle}{E_e - E_0 + \varepsilon_k^e - \varepsilon_i^0 - \hbar\omega_L} \quad (18)$$

represents a good approximation in the neighborhood of resonances<sup>36,55-57</sup>. Eq. (18) also shows that in case of a single, isolated resonance, as it is often present in organic chromophors, the Raman cross section is mainly determined by the weighted Franck-Condon overlaps  $\langle i^0 | k^e \rangle \langle k^e | f^0 \rangle$  corresponding to this single transition.<sup>23</sup>

Albrecht<sup>27</sup> splits the contributions of the first derivatives in (16) into a resonant part (*B* term)

$$V_{FI}^B = \sum_e \sum_k \mathbf{u}_L \cdot \frac{\langle i^0 | k^e \rangle \langle k^e | Q_v | f^0 \rangle \mathbf{m}_e \mathbf{m}_e^{v*} + \langle i^0 | Q_v | k^e \rangle \langle k^e | f^0 \rangle \mathbf{m}_e^v \mathbf{m}_e^*}{E_e - E_0 + \varepsilon_k^e - \varepsilon_i^0 - \hbar\omega_L} \cdot \mathbf{u}_S \quad (19)$$

and a non-resonant part (*C* term)

$$V_{FI}^C = \sum_e \sum_k \mathbf{u}_L \cdot \frac{\langle i^0 | k^e \rangle \langle k^e | Q_v | f^0 \rangle \mathbf{m}_e^{v*} \mathbf{m}_e + \langle i^0 | Q_v | k^e \rangle \langle k^e | f^0 \rangle \mathbf{m}_e^* \mathbf{m}_e^v}{E_e - E_0 + \varepsilon_k^e - \varepsilon_i^0 + \hbar\omega_S} \cdot \mathbf{u}_S, \quad (20)$$

where the shorthand  $\mathbf{m}_e^v = \partial \mathbf{m}_e / \partial Q_v$  is used. The sum of these two terms are labeled Albrecht *B* term by Gong et al<sup>30</sup> and is also called Franck-Condon/Herzberg-Teller term<sup>31,54</sup>. There is also the possibility to consider both derivatives in the matrix elements. This so called Herzberg-Teller term<sup>31</sup> is believed to be only important when the matrix elements vanish, i.e. for symmetry forbidden transitions<sup>58</sup> and is not considered in our work.

In order to simplify the dependence on the polarization vectors  $\mathbf{u}_L$  and  $\mathbf{u}_S$ , the so called

Raman invariants<sup>1</sup> can be defined from the tensor elements of  $\alpha' = \partial\alpha/\partial Q_v$  for the Placzek approximation. These are the mean polarizability<sup>1,3,59</sup>

$$a = \frac{1}{3}(\alpha'_{xx} + \alpha'_{yy} + \alpha'_{zz}), \quad (21)$$

the anisotropy<sup>1,31</sup> (this quantity is also denoted by  $\beta^{3,49}$  or  $g^{36}$ )

$$\begin{aligned} \gamma^2 = \frac{1}{2} [ & |\alpha'_{xx} - \alpha'_{yy}|^2 + |\alpha'_{xx} - \alpha'_{zz}|^2 + |\alpha'_{yy} - \alpha'_{zz}|^2 ] + \\ & \frac{3}{4} [ |\alpha'_{xy} + \alpha'_{yx}|^2 + |\alpha'_{xz} + \alpha'_{zx}|^2 + |\alpha'_{yz} + \alpha'_{zy}|^2 ] \end{aligned} \quad (22)$$

and the asymmetric anisotropy<sup>1</sup> (often assumed to vanish<sup>3,49</sup> as expected for non-resonant Raman<sup>2</sup>, and also denoted by  $d^{36}$ )

$$\delta^2 = \frac{3}{4} [ |\alpha'_{xy} - \alpha'_{yx}|^2 + |\alpha'_{xz} - \alpha'_{zx}|^2 + |\alpha'_{yz} - \alpha'_{zy}|^2 ] \quad (23)$$

from which the absolute Raman intensity<sup>3,16,36,49</sup>

$$I_{\text{Ram},v} = 45a^2 + 7\gamma^2 + 5\delta^2 \quad (24)$$

is obtained. This intensity is usually given in units of  $\text{\AA}^4/\text{amu}$ .<sup>3</sup> Expression (24) is valid only for the most common experimental setup and other combinations of  $a, \gamma, \delta$  appear depending on the polarization of incoming and outgoing photons.<sup>1</sup> Similar Raman invariants can also be defined from the tensor element of the matrix element (4) instead of the polarizability derivatives  $\alpha'$ .<sup>1</sup> The resulting expression for the intensity is similar to (24) and is called  $I$  in the following. In order to directly compare  $I$  and  $I_{\text{Ram},v}$  one would have to multiply the latter with the vibrational matrix element (Franck-Condon factor)  $|\langle i^0 | Q_v | f^0 \rangle|^2$ . The intensity  $I$  is therefore usually given in  $(\text{e}\text{\AA}/\text{eV})^2$ .

In the following, we will compare Placzek and Albrecht approximations using ab-initio

calculations of small molecules. This will show the similarities and differences of the two approximations. We will find that the Albrecht and its semi-classical approximation Placzek largely agree for all excitation frequencies and that in particular the approximation of Profeta corresponds to Albrecht B/C and the missing terms Pl/Pr to Albrecht A. The interested reader is also referred to Appendix A that elaborates on a clear connection between Placzek and Albrecht in the limit  $\omega_L \rightarrow 0$ .

### 3 Methods

The electronic structure of the systems considered here is described by density functional theory (DFT) as implemented in the GPAW software suite<sup>60,61</sup>. The Kohn-Sham orbitals and the electronic density are described in the projector augmented wave (PAW) method<sup>62</sup> where the smooth wave functions are represented on real space grids. The exchange correlation functional is approximated in the generalized gradient correction as devised by Perdew, Burke and Ernzerhof (PBE)<sup>63</sup>. The real space grid was ensured to contain at least 4 Å of vacuum space around each atom. The grid spacing for the wave-functions was chosen to be 0.2 Å, while the density was represented on grids with 0.1 Å spacing. Molecular structures were considered to be relaxed when no force exceed 0.01 eV/Å. Vibrational modes and frequencies are calculated within the finite difference approximation of the dynamical matrix<sup>3,64</sup>. Excited state properties are calculated in time dependent DFT (TDDFT) linear response formalism as reported by Casida<sup>65,66</sup>. The range of Kohn-Sham single-particle excitations was large enough to cover all the excitations in the energy ranges displayed, which also ensures convergence of the sum over states in polarizability derivatives and Albrecht terms. The Franck-Condon factors are calculated as described by Guthmuller.<sup>31</sup>

We use the IMDHO approximation that considers only changes in excited state energies in linear order and no mixing of ground state vibrational modes, i.e. Duschinsky effects<sup>31</sup> are thus not included. Derivatives of polarizabilities, transition energies and matrix elements

are calculated using finite differences. Note, that this involves arbitrary phases related to the Berry phase in case of the matrix elements from eq. (16) and therefore needs special care as discussed in appendix C.

## 4 Results

Molecular hydrogen is the simplest existing neutral molecule and serves as a good example to show the basic properties and consequences of the different approximations for obtaining Raman intensities described above. There is only one vibrational mode in  $\text{H}_2$  which is found in our calculation at  $4337 \text{ cm}^{-1} = 0.538 \text{ eV}$  in fair agreement to the exact value of  $4163.3 \text{ cm}^{-1}$ .<sup>67</sup>

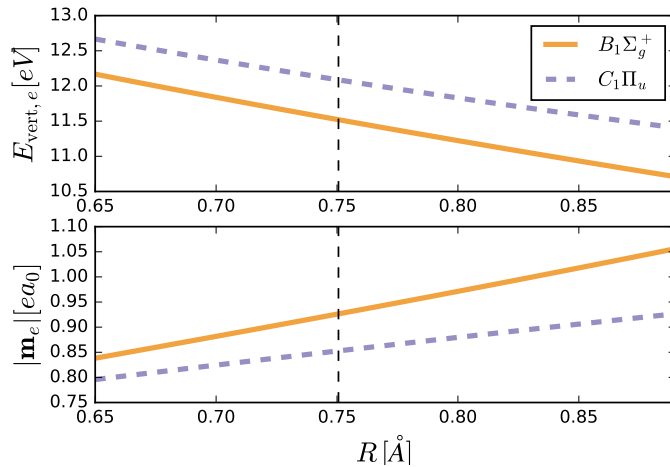


Figure 2: Electronic transition energies  $E_{\text{vert},e}$  and transition dipoles from the ground  $^1\Sigma_u^+$  state to  $B^1\Sigma_g^+$ ,  $C^1\Pi_u$  states of the  $\text{H}_2$  molecule depending on the nuclear distance  $R$ . Vertical lines indicate the equilibrium distance.

The main ingredients determining Raman intensities are the derivatives of transition energy and dipole matrix element with respect to the normal coordinate of the corresponding vibration in Eqs. (11) and (16). Fig. 2 shows these quantities for the first two optically allowed transitions in the  $\text{H}_2$  molecule in dependence of the bond length  $R$ . Both quantities depend linearly on  $R$  in agreement with the literature<sup>68,69</sup>. Adding a linear function to a

Harmonic potential does only change the potential minimum, but not its form, i.e. the vibrational frequencies in ground and excited state are the same (see also appendix B). Therefore the displaced harmonic oscillator model underlying the definition of the Huang-Rhys parameter<sup>70</sup> is indeed justified here. Taking into account only the linear term in a Taylor expansion of the energy around the equilibrium position in the normal modes leads to the displaced harmonic oscillator model depicted in Fig. 1.

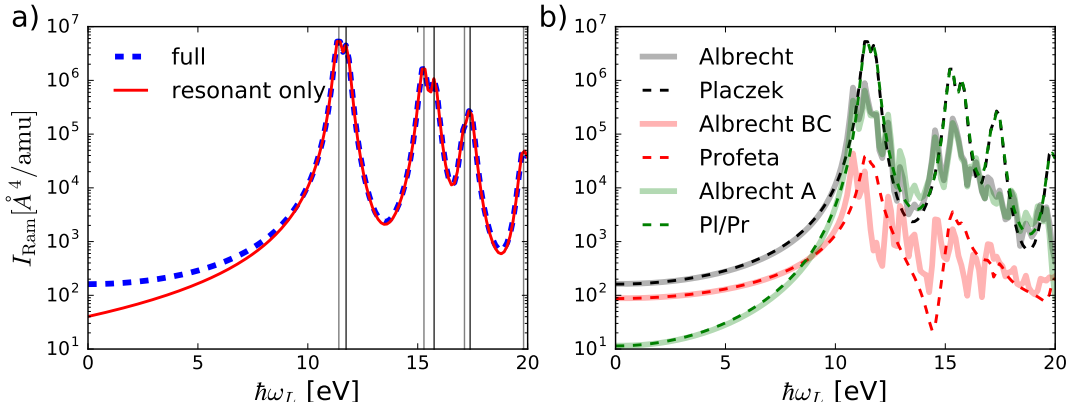


Figure 3: a) Full Placzek Raman intensity for  $\text{H}_2$  compared to the resonant term only. Vertical lines show optically active transitions with oscillator strength  $f \geq 0.01$ . b) Raman intensity from different approximations. A width of  $\gamma = 0.2$  eV is applied for Placzek like approximations and  $\gamma = 0.1$  eV for Albrecht terms.

Fig. 3 a) shows the absolute Raman intensity in logarithmic scale as a function of the excitation frequency  $\omega_L$ . The Raman intensity displays a rather smooth dependence on photon energy for small  $\hbar\omega_L$ , i.e. if  $\hbar\omega_L \ll E_e$  for all optically strong electronic transition energies  $E_e$  in the system. In contrast, the intensity gets strongly peaked close to the transition energies if there is sufficient oscillator strength in the corresponding transitions. A finite width  $\gamma$  is added as complex energy to the full range of  $\hbar\omega_L$  effectively broadening these peaks. Fig. 3 a) also compares the contributions of the resonant and non-resonant terms in eq. (8). The non-resonant part can indeed be neglected, except when approaching the static limit  $\hbar\omega_L \rightarrow 0$ , where the non-resonant part is needed to get full intensity.

A comparison of the different approximations and their contributions for  $\text{H}_2$  is depicted in Fig. 3 b). We report the absolute Raman intensity although the Albrecht terms do not

contain the factor  $|\langle i^0 | Q_v | f^0 \rangle|^2$  in eq. (12). The Albrecht matrix elements have been divided by this factor to get comparable numbers. Concentrating on the full Albrecht and Placzek approximation first, the similarity and even overlap of the two approximations for small  $\omega_L$  far from the resonances becomes apparent. The two approximations yield the same result in a wide energy range and there is even a qualitative similarity in the resonance regions. The main difference is that the less approximate Albrecht approximation leads to many more peaks than Placzek. The Placzek peaks are at the semi-classical vertical transition energies where the denominator in eq. (8) diverges. In contrast, the Albrecht terms exhibit peaks at each of the phonon decorated electronic excitations in the denominators of A, B and C terms in Eqs. (17-20). For this reason we had to apply twice the broadening  $\gamma$  in the narrower peaks of Placzek as compared to Albrecht.

Table 1: Static ( $\omega_L = 0$ ) absolute Raman intensities for the H<sub>2</sub> molecule in Å<sup>4</sup>/amu.

	full	Albrecht A or Pl/Pr	Albrecht BC or Profeta
Albrecht	191	11.5	109
Placzek	188	11.4	107

Interestingly, and in agreement with the considerations of appendix A, the Profeta approximation turns out to be the semi-classical approximation of the Albrecht BC terms. The term missing in Profeta treatment corresponds to the Albrecht A term. The connections and agreement between Albrecht and Placzek, and Albrecht BC and Profeta are further corroborated by the numerical values for static Raman intensities listed in tab. 1. As expected, the Albrecht BC terms dominate for small  $\omega_L$ , but these terms are not enough to give the full intensity. Even in the limit  $\hbar\omega_L/E_e \rightarrow 0$  the consideration of the Albrecht A contribution is important and cannot be neglected. Albrecht A clearly dominates in the resonance region and is the main contribution to the full Raman intensity. In certain energy regions the Albrecht A intensity is even larger than full Albrecht, which indicates destructive interference with the Albrecht BC terms. We note that there is no energy region where Albrecht BC (and Profeta) is sufficient to give the correct intensities. Placzek generally provides a good

coarse grained description of the intensity behavior as compared to Albrecht, however.

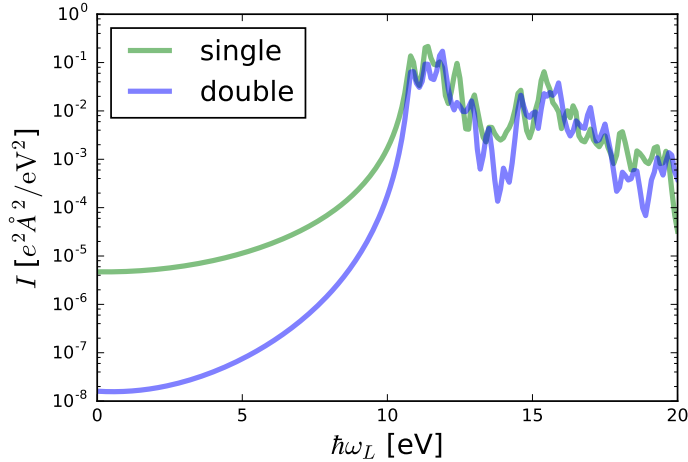


Figure 4: Single and double vibrational excitation intensities according to the Albrecht A term in the  $\text{H}_2$  molecule. A width of  $\gamma = 0.1$  eV is applied.

Now we turn to multiple vibrational excitations, the so called overtones and combinations bands in contrast to the fundamentals that correspond to single excitations.<sup>42</sup> Here, we expect severe difference between Albrecht and Placzek approximations since they are impossible in Placzek within the IMDHO approximation. As an example, the intensity of double vibrational excitation in the Albrecht A term of  $\text{H}_2$  is compared to the single excitation Albrecht A term in Fig. 4. For low excitation energies and thus far from resonance, the intensity of vibrational double excitation is several orders of magnitude smaller than that of a single excitation. This changes drastically near to resonances, where the intensities become the same size and the intensity of the vibrational double excitation can even overbalance that of the single excitation.

Table 2: Vibrational frequencies in  $\text{cm}^{-1}$  and Placzek absolute Raman intensities for  $\hbar\omega_L/E_e \rightarrow 0$  in  $\text{\AA}^4/\text{amu}$ . A width of  $\gamma = 0.2$  eV is applied for the calculations at  $\omega_L^{\text{exp}}$ .

mode	$\omega_v$		$I_{\text{Ram}}(0)$		$I_{\text{Ram}}(\omega_L^{\text{exp}} \equiv 514.5\text{nm})$		
	ours	exp.	ours	others	ours	others	exp. <sup>f</sup>
$v_2(1A_1)$	1585	1595 <sup>a</sup> , 1638 <sup>b</sup>	1.4	0.8 <sup>c</sup> , 0.9 <sup>d</sup> , 1.1 <sup>e</sup>	1.4	1.1 <sup>e</sup>	$0.9 \pm 0.2$
$v_1(2A_1)$	3747	3657 <sup>a</sup> , 3832 <sup>b</sup>	112	109 <sup>c</sup> , 120 <sup>d</sup> , 111 <sup>e</sup>	127	129 <sup>e</sup>	$108 \pm 14$
$v_3(1B_2)$	3846	3756 <sup>a</sup> , 3943 <sup>b</sup>	25	26 <sup>c</sup> , 30 <sup>d</sup> , 26 <sup>e</sup>	28	29 <sup>e</sup>	$19.2 \pm 2.1$

<sup>a</sup>exp. vapor<sup>71</sup>, <sup>b</sup>exp. harmonic<sup>72</sup>, <sup>c</sup>PW92<sup>3</sup>, <sup>d</sup>BP86<sup>73</sup>, <sup>e</sup>PBE<sup>74</sup>, <sup>f</sup>from ref.<sup>47</sup>

Next we consider the water molecule. We first discuss the results in the limit  $\hbar\omega_L/E_e \rightarrow 0$  where several other calculations and extensive experimental data (for small  $\hbar\omega_L$ ) are available. The gas-phase water molecule has three independent vibrational modes that are all Raman active. Table 2 shows the good agreement of our calculated absolute Raman intensities in this limit both with experiment as well as with other calculations. There are differences due to different density functionals applied, but all approaches are of roughly the same good accuracy as compared to experiment. Static and dynamic polarizabilities for the experimental wavelength of 514.5 nm (2.41 eV) lead to small differences<sup>74</sup>, only. While the very weak Raman intensity of  $v_2$  does not change, the stronger  $v_1$  and  $v_3$  slightly increase. Table 3 lists the static ( $\omega_L \rightarrow 0$ ) absolute Raman contributions from the Albrecht terms.

Table 3: Absolute Raman intensities for  $\omega_L = 0$  in the Albrecht approximations from our calculations and from Gong et al.<sup>30</sup> in  $\text{\AA}^4/\text{amu}$ .

mode	exp <sup>47</sup>	Albrecht	Albrecht <sup>30</sup>	Albr. $A$	Albr. $A^{30}$	$B + C$	$B + C^{30}$
$v_2$	0.9	2.7	1.1	0.5	0.1	5.3	1.5
$v_1$	108	103	105	7.6	11.7	56	48.3
$v_3$	19.2	30	25.7	0	0	30	25.7

Our calculation agrees well with the the recent results of Gong et al.<sup>30</sup> and we confirm that the Albrecht A term cannot be neglected in this limit for  $v_1$  and  $v_2$ .

Next we increase the energy of the incoming photon to the resonance region as shown in Fig. 5, where  $I_{\text{Ram}}$  is depicted on logarithmic scale in the region up to 20 eV. There are dramatic changes in the relative intensities. Coming from small  $\omega_L$  all three vibrations show increasing intensity when entering the resonance region. The behavior of the three vibrations is very different, however. While  $v_1$  and  $v_2$  show a clear peak at the first optically active transition,  $v_3$  is unaffected. Interestingly, vibration  $v_1$ , that is extremely weak in the limit  $\omega_L \rightarrow 0$  increases most rapidly and even gets the highest contribution around 9 eV. The deep minima in the intensities visible in particular for  $v_3$  indicate destructive interference that strongly affects the intensity.

Finally we present the non-resonant and near-resonant Raman spectra of trans-butadiene



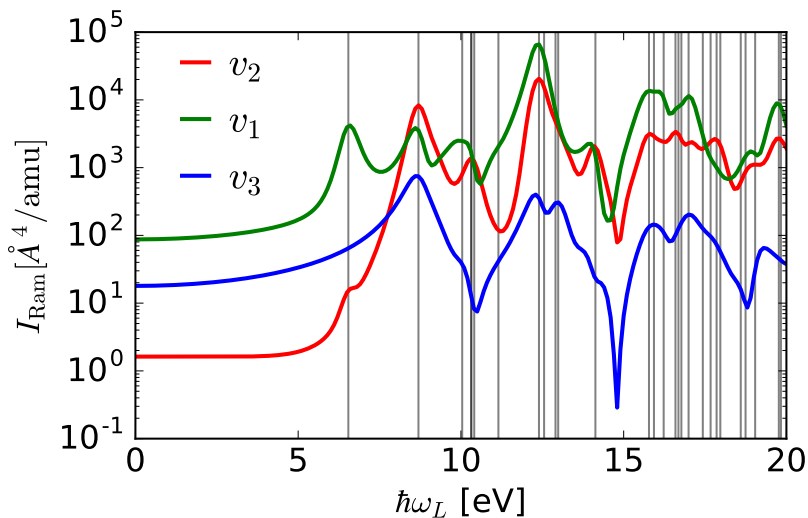


Figure 5: Frequency dependent Placzek-Raman intensities of the three vibrations in water. A width of  $\gamma = 0.2$  eV is applied. Optically active transitions with  $f \geq 0.02$  are marked by gray lines.

where experimental non-resonant<sup>75</sup> resonant<sup>76</sup> Raman spectra as well as an early theoretical investigation within the Albrecht approximation<sup>25</sup> are available. Duschinsky effects have been reported in this molecule<sup>77</sup> and these are important to understand the fluorescence quantum efficiency.<sup>78,79</sup> The neglect of mode mixing as in the IMDHO model applied here has been reported to capture the geometry changes in the main optical  $1^1A_g^- \rightarrow 1^1B_u^+$  transition,<sup>80</sup> however. In the experiment this transition is found at 5.92 eV. Our calculated value (5.53 eV) is lower than the experimental one as well as the transition energy in higher level quantum chemistry methods<sup>81</sup>. The oscillator strength is 0.68, which is higher than the experimental value of 0.4<sup>82</sup>, but in concord with other computations<sup>82</sup>. The underestimation of excitation energies in GGAs is well known<sup>83</sup>, while the rather accurate oscillator strength indices a qualitatively correct description of the nature of the excitation. In order to compare our resonant Raman calculations to experiment we have to take account of the differences in excitation energies. Multiple vibrational excitations appear only if there is a nearby resonance and their contribution crucially depends on the energetic distance between  $\hbar\omega_L$  and  $E_I$  as we have seen in Fig. 4 for H<sub>2</sub>. In the following we calculate our spectra at 5.92

eV - 5.53 eV = 0.39 eV lower excitation energies than in experiment in order to be at the same energetic distance from the main optical resonance.

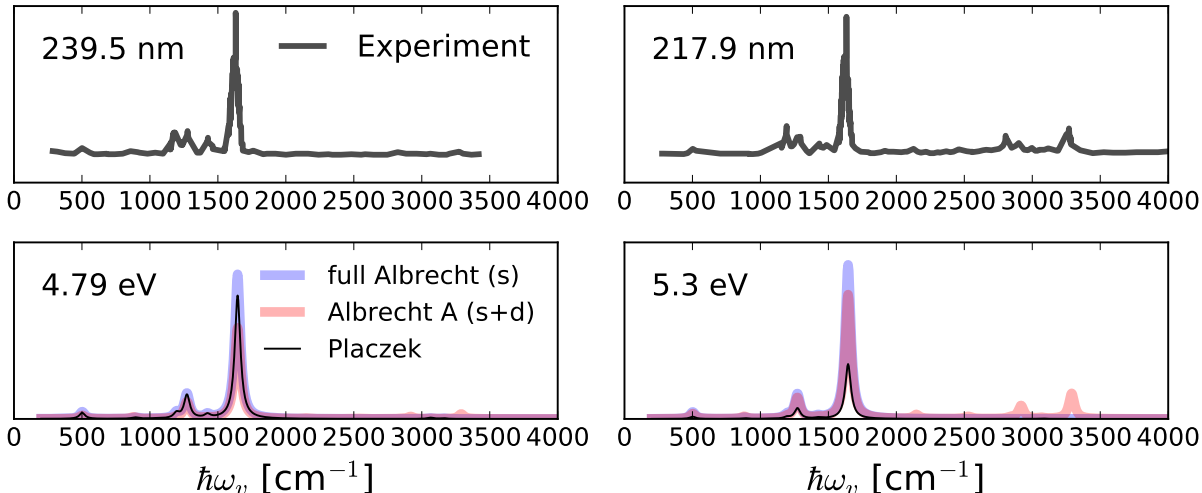


Figure 6: Near resonant ( $\hbar\omega_L = 5.3$  eV  $\hat{=}$  217.9 nm, see text) and more off-resonant ( $\hbar\omega_L = 4.79$  eV  $\hat{=}$  239.5 nm) Raman spectra for trans-butadiene in comparison to the experimental spectra of Chadwick et al.<sup>76</sup> The spectrum labeled full Albrecht (s) contains all Albrecht A-C terms for single vibrational contributions, while the Albrecht A (s+d) term contains vibrational double excitations also. A width of  $\gamma = 0.2(0.4)$  eV was applied to Albrecht(Placzek) approximations and the intensities were folded by Lorentzians of  $50$   $\text{cm}^{-1}$  width.

Experimental and calculated spectra related in this way closely resemble each other as is shown in Fig. 6. The spectrum in the non-resonant region (at 4.79 eV in our calculation corresponding to 239.5 nm or 5.18 eV experimentally) has significant contribution from the Albrecht B and C terms and there is nearly no intensity above  $2000$   $\text{cm}^{-1}$ . In this frequency range the Placzek approximation gives a good description of the spectrum. Apart from the main peak at  $1645$   $\text{cm}^{-1}$  also other small peaks at lower vibrational energies appear in the calculation similar to experiment as further detailed in Tab. 4 below. This changes near to resonance (5.30 eV in our calculation corresponding to 217.9 nm or 5.69 eV experimentally), where Albrecht A practically determines the full intensity. The Placzek approximation gives much lower intensity as compared to Albrecht. There are also contributions of higher excitations due to the dominating Albrecht A term that naturally appear at higher vibrational

frequencies. These are completely neglected within the Placzek approximation.

Table 4: Vibrational energies (in  $\text{cm}^{-1}$ ) and relative intensities of the most active Raman lines. The intensity of the strongest line in  $e^4 \text{\AA}^4 / \text{eV}^2$  is given in brackets. Assignment of modes follows Chadwick et al.<sup>76</sup>, and  $\beta, \gamma$  represent in-plane bending and stretching modes, respectively. Numerical settings as in Fig. 6.

$\hbar\omega_v$	$\hbar\omega_v$ (exp)	assignment	$I^{\text{Albrecht}}$	$I^{\text{Placzek}}$	$I^{\text{AlbrechtA}}$	$I^{\text{Albrecht,c}}$
502	513 <sup>a</sup> , 508 <sup>b</sup>	$v_9 \beta(\text{CCC})$	4.1	3.8	3.9	0.2
879	910 <sup>a</sup> , 890 <sup>b</sup>	$v_8 \gamma(\text{C-C}), \beta(\text{H})$	0.8	1.1	1.9	1.3
1195	1204 <sup>a</sup> , 1200 <sup>b</sup>	$v_7 \gamma(\text{C-C})$	2.3	3.0	1.4	40.3
1272	1279 <sup>a</sup> , 1279 <sup>b</sup>	$v_6 \beta(\text{H})$	14.1	16.9	15	0.7
1275		$\beta(\text{H})$	1.4	1.8	1.4	-
1424	1442 <sup>a</sup> , 1442 <sup>b</sup>	$v_5 \beta(\text{H})$	1.3	1.7	0.7	0.3
1645	1643 <sup>a</sup> , 1642 <sup>b</sup>	$v_4 \gamma(\text{C-C}, \text{C}=\text{C})$	100(0.87)	100(0.31)	100(0.7)	100
2917	2879 <sup>a</sup>	$v_4 + v_6$	-	-	10.7	-
3290	3267 <sup>a</sup>	$2v_4$	-	-	23.2	-

<sup>a</sup>experiment of Richards and Nielsen<sup>75</sup>, <sup>b</sup>experiment of Chadwick et al.<sup>76</sup>, <sup>c</sup> non-resonant ( $\hbar\omega_L = 1.24 \text{ eV}$ ) Albrecht from Warshel and Dauber<sup>25</sup>

The Raman peaks and their intensities are further detailed in tab. 4. As suggested from Fig. 6 our vibrational energies are in good agreement to experiment. There are two in-plane H-bending modes at  $1272 \text{ cm}^{-1}$  and  $1275 \text{ cm}^{-1}$  that are probably hard to resolve in the experiment. One of them is the second most intense line in our calculations, while the strong Raman excitation of the  $1195 \text{ cm}^{-1}$  found in the calculations of Warshel and Dauber<sup>25</sup> cannot be confirmed by us (further off-resonant spectra resemble the 4.79 eV spectrum in Fig. 6). Interestingly, the Placzek approximation gives relative intensities in good agreement to Albrecht despite its much lower absolute intensity.

## 5 Conclusions

We have shown in this contribution how the Placzek and Albrecht terms can be derived from the photon scattering matrix elements in the formulation by Kramers, Heisenberg and Dirac. The widely used Placzek approximation is found to represent the semi-classical limit of the more exact Albrecht formulation. While the excitation energy-dependent peak structure is

much simpler in the Placzek approximation, the overall behavior of the Raman intensities is remarkably similar to Albrecht also in resonance regions for the molecules investigated. The similarity breaks down for multiple excitations of vibrational modes appearing as soon as the photon energy approaches the resonance region. These are forbidden in the Placzek form within the independent mode double harmonic approximation, but are well described within the Albrecht approximation.

## 6 Acknowledgment

MW thanks J. Guthmuller for useful discussion. Support by ASTC is gratefully acknowledged. We are grateful for computational resources from FZ-Jülich and from the Nemo cluster at the University of Freiburg.

## A Connection between Placzek and Albrecht approximations for $\omega_L \rightarrow 0$

We consider the limit of very small excitation energies  $\hbar\omega_L$ , where small means far from any electronic resonance in the system. This limit can formally be described by  $\omega_L \rightarrow 0$ . However, this is a formal limit only, as scattering of zero frequency photons is meaningless. Both Placzek and Albrecht approximations should be valid in this limit and the approximations indeed coincide as we will show in the following.

The polarizability tensor (10) in this limit simplifies to<sup>46</sup>

$$\alpha(\omega = 0) = \sum_e \frac{2m_L^e m_S^e}{E_{\text{vert},e}}. \quad (25)$$

This tensor enters the Placzek approximation via its derivatives with respect to vibrational coordinates. Nonzero derivatives arise from two distinct sources: Either from the transition

energy  $E_{\text{vert},e}$  or from the matrix elements  $m_{L,S}^e$ . Without loss of generality, we consider only a single electronic excited state and thus suppress the label  $e$  for brevity in the following. The explicit derivative is then

$$\frac{\partial \alpha}{\partial Q} = \frac{2}{E_{\text{vert}}} [m_S m'_L + m_L m'_S] - 2m_S m_L \frac{E'_{\text{vert}}}{E_{\text{vert}}^2}, \quad (26)$$

where the prime denotes the derivative with respect to a nuclear coordinate.

In order to show the equivalence to the Albrecht approximation for  $\omega_L \rightarrow 0$ , we will discuss the different terms appearing in (26) separately and show that these correspond to the different terms in the Albrecht approximation, i.e. we will show that in the limit of small  $\omega_L$

$$V^A \approx -\langle 0^0 | Q | 1^0 \rangle 2m_S m_L \frac{E'_{\text{vert}}}{E_{\text{vert}}^2} \quad (27)$$

and

$$V^B + V^C \approx \langle 0^0 | Q | 1^0 \rangle \frac{2}{E_{\text{vert}}} [m_S m'_L + m_L m'_S] \quad (28)$$

hold.

We first discuss the Albrecht B term, defined by eq. (19), which becomes in the limit of  $\hbar\omega_L/E \rightarrow 0$

$$V^B = m_S m'_L \sum_k \frac{\langle 0^0 | Q | k \rangle \langle k | 1^0 \rangle}{E + k\varepsilon} + m_S m'_L \sum_k \frac{\langle 0^0 | k \rangle \langle k | Q | 1^0 \rangle}{E + k\varepsilon} \quad (29)$$

Replacing the denominator  $E + k\varepsilon$  by the vertical transition energy  $E_{\text{vert}}$  and applying the completeness relation eq. (7) leads to

$$V^B = \frac{1}{E_{\text{vert}}} [m_S m'_L + m_L m'_S] \langle 0^0 | Q | 1^0 \rangle \quad (30)$$

which is the half of the first term in eq. (28). The other half is given by  $V^C$  within the same approximation.

To prove (27) we consider real matrix elements

$$V^A = m_L m_S \sum_k \langle 0^0 | k \rangle \langle k | 1^0 \rangle \left[ \frac{1}{E + k\varepsilon - \omega_L} + \frac{1}{E + k\varepsilon + \omega_S} \right], \quad (31)$$

use  $\omega_S \approx \omega_L$ ,  $\omega_L \rightarrow 0$  and expand in  $\varepsilon/E$  up to first order, which leads to

$$V^A = 2m_L m_S \sum_k \langle 0^0 | k \rangle \langle k | 1^0 \rangle \frac{1}{E} \left( 1 - k \frac{\varepsilon}{E} \right) \quad (32)$$

The first term in brackets vanishes due to orthogonality of  $\langle 0^0 | 1^0 \rangle$  (after closure in  $k^e$ ) and one can show that

$$\sum_k \langle 0^0 | k \rangle k \langle k | 1^0 \rangle = -\frac{\Delta}{\sqrt{2}} \quad (33)$$

where the dimensionless displacement

$$\Delta = \sqrt{\frac{\mu\omega}{\hbar}} \left( \xi_0^{(e)} - \xi_0^{(0)} \right) \quad (34)$$

appears (c.f. Fig. 1). One can further show that

$$\langle 0^0 | Q | 1^0 \rangle E'_{\text{vert}} = \sqrt{\frac{\hbar}{2\omega}} \left( -\varepsilon \Delta \sqrt{\frac{\omega}{\hbar}} \right) \quad (35)$$

such that eq. (32) can be written

$$V^A \approx -2m_L m_S \frac{E'_{\text{vert}}}{E_{\text{vert}}^2} \quad (36)$$

where  $E \approx E_{\text{vert}}$  entered. This finally proves the approximate equality of Placzek and Albrecht approximations in the limit  $\omega_L \rightarrow 0$ .

## B Taylor expansion and displaced harmonic oscillator

Franck-Condon factors can be efficiently calculated within the double harmonic approximation. Deviations from this approximation, the Herzberg-Teller and Duschinsky effects are usually rather small<sup>84</sup>. This property can be understood by expanding the possible effects in a series in the displacement between ground and excited state equilibria  $\rho_0$  and  $\rho_e$  of some vibrational coordinate  $\rho$ . The ground state potential in the harmonic approximation is given by

$$E_0(\rho) = E_0(\rho_0) + \frac{1}{2}\mu\omega^2(\rho - \rho_0)^2, \quad (37)$$

where  $\mu$  is the effective mass and  $\omega$  the corresponding frequency of the harmonic potential. We may expand the excited state energy around  $\rho_0$  in a Taylor series up to first order

$$E_e(\rho) = E_e(\rho_0) + \left. \frac{\partial E_e(\rho)}{\partial \rho} \right|_{\rho=\rho_0} (\rho - \rho_0) + O[(\rho - \rho_0)^2] \quad (38)$$

Adding Eqs. (37) and (38) immediately leads to the similar harmonic equation in the excited state

$$E_e(\rho) = E_e(\rho_0) + \frac{1}{2}\mu\omega^2(\rho - \rho_e)^2 \quad (39)$$

where we have identified  $\rho_e = \rho_0 - \frac{\partial E_e(\rho)}{\partial \rho}/(\mu\omega^2)$ . Thus the leading term in eq. (38) changes the equilibrium position, but not the vibrational frequency<sup>85</sup>.

## C Matrix element derivatives and the Berry phase

The evaluation of Albrecht B and C terms requires derivatives of transition dipoles with respect to nuclear coordinates. An evaluation of such derivatives in finite differences is not straightforward as it involves arbitrary phases that are present in eigenstates of parameter

dependent Hamiltonians and are connected to the Berry phase<sup>86,87</sup>. Similar problems are also present in the evaluation of hopping matrix elements<sup>88</sup>.

The nature of the problem and its solution can be exemplified in one dimension involving a single electronic positional coordinate  $x$ . An electron might be subject to a parameter dependent Hamiltonian  $H(R)$ , where in  $R$  in our case is a nuclear coordinate. The aim is to calculate the derivative of an normalized eigenstate  $f_i(x; R)$  of  $H(R)$  with respect to the  $R$  in a finite difference expression

$$dR \frac{\partial f_i(x; R)}{\partial R} = f_i(x; R + dR) - f_i(x; R) . \quad (40)$$

In practical calculations the evaluation of eigenstates at different  $R$  are independent of each other<sup>88</sup>. Then every eigenstate  $\bar{f}_i(x; R + dR) = u f_i(x; R + dR)$  with  $|u|^2 = 1$  is a perfectly valid eigenstate of  $H(R + dR)$  and equally relevant as  $f_i(x; R + dR)$  itself. The phase  $u$  can spoil the derivative if  $\bar{f}$  is used instead of  $f$  in expression (40), however. To recover  $f_i(x; R + dR)$  we have to apply

$$dR \frac{\partial f_i(x; R)}{\partial R} = u^* \bar{f}_i(x; R + dR) - f_i(x; R) \quad (41)$$

instead, where we correct for the arbitrary phase  $u$ . The value of this phase factor is reconstructed by using the orthogonality of  $f_i$  and  $\partial f_i / \partial R$ <sup>86</sup> that is required for normalized states. It leads to

$$u = \int dx f^*(x; R) \bar{f}(x; R + dR) . \quad (42)$$

We have to be slightly more careful in the case of energetically degenerate states, that are common in molecules. Here, not only a phase  $u$  may appear, but the states may also mix. More generally we are faced with

$$\bar{f}_i(x; R + dR) = \sum_j u_{ij} f_j(x; R + dR) \quad (43)$$



where the matrix  $u$  is unitary, but arbitrary otherwise. It might be sparse, but generally not diagonal. Similar to (42) the matrix elements of  $u$  can be reconstructed from

$$u_{ij} = \int dx f_j^*(x; R) \bar{f}_i(x; R + dR) \quad (44)$$

when terms containing  $dR$  are neglected, i.e. we assume that the matrix  $u$  does not change due to the small displacement. This leads to the generalized finite difference equation save from arbitrary phases

$$dR \frac{\partial f(x; R)}{\partial R} = u^H \bar{f}(x; R + dR) - f(x; R) . \quad (45)$$

where  $f$  is the vector of eigenstates  $f_i$ ,  $\bar{f}$  is the vector of eigenstates  $\bar{f}_j$  and the superscript  $H$  denotes the Hermitian conjugate.

Similar to the Eigenstates discussed so far, we want to obtain derivatives of transition dipole matrix elements  $m_{i\alpha}(R) = \langle f_i(x; R) | \hat{o} | f_\alpha(x; R) \rangle$  in a finite difference expression through

$$dR \frac{\partial m_{i\alpha}(R)}{\partial R} = m_{i\alpha}(R + dR) - m_{i\alpha}(R) , \quad (46)$$

where  $i, \alpha$  are the indices of occupied and empty orbitals, respectively. The transition dipoles are calculated in an independent calculation again and thus are mixed and contain arbitrary phases inherited from the orbitals. We may correct for this similar to eq. (45) and write

$$dR \frac{\partial m_{i\alpha}(R)}{\partial R} = \langle [u^H \bar{f}(R + dR)]_i | \hat{o} | [u^H \bar{f}(R + dR)]_\alpha \rangle - m_{i\alpha}(R) \quad (47)$$

or in vector form

$$dR \frac{\partial m(R)}{\partial R} = U^H \bar{m}(R + dR) - m(R) \quad (48)$$

with

$$U_{i\alpha, j\beta} = u_{ij}^* u_{\alpha\beta} \quad (49)$$

and  $\bar{m}_{i\alpha}(R + dR) = \langle \bar{f}_i(x; R + dR) | \hat{\rho} | \bar{f}_\alpha(x; R + dR) \rangle$ .

A new class of phases appears in linear response TDDFT where the eigenvalue equation<sup>66,89</sup>

$$\Omega F_I = \omega_I^2 F_I \quad (50)$$

is solved at each position independently. The  $\omega_I$  denote transition energies and the eigenvectors  $F_I$  may contain arbitrary phases and might be mixed. The matrix elements are then

$$M_I = \sum_{i\alpha} \sqrt{\frac{\varepsilon_\alpha - \varepsilon_i}{\omega_I}} (F_I)_{i\alpha} m_{i\alpha} \quad (51)$$

with the single particle energies  $\varepsilon_{i,\alpha}$ . The  $F_I$  at equilibrium position and the  $\bar{F}_J$  at a displaced position are given in the corresponding particle-hole basis that we may contract to single indices  $p = (i\alpha), q = (j, \beta)$  to simplify the notation. We may define an overlap similar to Eqs. (44) and (49)

$$W_{IJ} = \sum_{p,q} (\bar{F}_J)_p U_{pq} (F_I)_q^* \quad (52)$$

where the  $U_{pq}$  are needed to connect the two particle-hole bases. This matrix connects the different linear response transition matrix elements via  $\bar{M} = WM$ , where

$$\bar{M}_I = \sum_{i\alpha} \sqrt{\frac{\varepsilon_\alpha - \varepsilon_i}{\omega_I}} (\bar{F}_I)_{i\alpha} \bar{m}_{i\alpha}. \quad (53)$$

Note, that the phases of  $\bar{F}$  and  $\bar{m}$  are both arbitrary and independent of each other. Derivatives of linear response dipole matrix elements are finally obtained as

$$dR \frac{\partial M(R)}{\partial R} = W^H \bar{M}(R + dR) - m(R). \quad (54)$$

## References

- (1) Derek A. Long, *The Raman Effect: A Unified Treatment of the Theory of Raman*

*Scattering by Molecules*; John Wiley & Sons Ltd, Baffins Lane, Chichester, West Sussex PO19 1UD, England, 2002.

- (2) John R. Ferraro,; Kazuo Nakamoto,; Chris W. Brown, *Introductory Raman Spectroscopy (Second Edition)*; Elsevier Inc., 2003.
- (3) Porezag, D.; Pederson, M. R. Infrared intensities and Raman-scattering activities within density-functional theory. *Physical Review B* **1996**, *54*, 7830–7836.
- (4) Yamakita, Y.; Kimura, J.; Ohno, K. Molecular vibrations of [n]oligoacenes (n=2-5 and 10) and phonon dispersion relations of polyacene. *The Journal of Chemical Physics* **2007**, *126*, 064904.
- (5) Castiglioni, C.; Tommasini, M.; Zerbi, G. Raman spectroscopy of polyconjugated molecules and materials: confinement effect in one and two dimensions. *Philosophical Transactions of the Royal Society of London A: Mathematical, Physical and Engineering Sciences* **2004**, *362*, 2425–2459.
- (6) Rouillé, G.; Jäger, C.; Steglich, M.; Huisken, F.; Henning, T.; Theumer, G.; Bauer, I.; Knölker, H.-J. IR, Raman, and UV/Vis Spectra of Corannulene for Use in Possible Interstellar Identification. *ChemPhysChem* **2008**, *9*, 2085–2091.
- (7) Zhao, L. L.; Jensen, L.; Schatz, G. C. Surface-Enhanced Raman Scattering of Pyrazine at the Junction between Two Ag<sub>20</sub> Nanoclusters. *Nano Letters* **2006**, *6*, 1229–1234.
- (8) Martin, E. J. J.; Bérubé, N.; Provencher, F.; Côté, M.; Silva, C.; Doorn, S. K.; Grey, J. K. Resonance Raman spectroscopy and imaging of push–pull conjugated polymer–fullerene blends. *Journal of Materials Chemistry C* **2015**, *3*, 6058–6066.
- (9) Vecera, P.; Chacón-Torres, J. C.; Pichler, T.; Reich, S.; Soni, H. R.; Görling, A.; Edelthalhammer, K.; Peterlik, H.; Hauke, F.; Hirsch, A. Precise determination of

- graphene functionalization by in situ Raman spectroscopy. *Nature Communications* **2017**, *8*, 15192.
- (10) Corni, S.; Cappelli, C.; Cammi, R.; Tomasi, J. Theoretical Approach to the Calculation of Vibrational Raman Spectra in Solution within the Polarizable Continuum Model. *The Journal of Physical Chemistry A* **2001**, *105*, 8310–8316.
- (11) Cheeseman, J. R.; Frisch, M. J. Basis Set Dependence of Vibrational Raman and Raman Optical Activity Intensities. *Journal of Chemical Theory and Computation* **2011**, *7*, 3323–3334.
- (12) Barone, V.; Biczysko, M.; Bloino, J. Fully anharmonic IR and Raman spectra of medium-size molecular systems: accuracy and interpretation. *Phys. Chem. Chem. Phys.* **2014**, *16*, 1759–1787.
- (13) Bloino, J.; Biczysko, M.; Barone, V. Anharmonic Effects on Vibrational Spectra Intensities: Infrared, Raman, Vibrational Circular Dichroism, and Raman Optical Activity. *The Journal of Physical Chemistry A* **2015**, *119*, 11862–11874.
- (14) Ambrosch-Draxl, C.; Auer, H.; Kouba, R.; Sherman, E. Y.; Knoll, P.; Mayer, M. Raman scattering in  $\text{YBa}_2\text{Cu}_3\text{O}_7$ : A comprehensive theoretical study in comparison with experiments. *Physical Review B* **2002**, *65*, 064501.
- (15) Gillet, Y.; Giantomassi, M.; Gonze, X. First-principles study of excitonic effects in Raman intensities. *Physical Review B* **2013**, *88*, 094305.
- (16) Li Niu,; Jiaqi Zhu,; Wei Gao,; Aiping Liu,; Xiao Han,; Shanyi Du, First-principles calculation of vibrational Raman spectra of tetrahedral amorphous carbon. *Physica B: Condensed Matter* **2008**, *403*, 3559–3562.
- (17) Wang, Y.; Carvalho, B. R.; Crespi, V. H. Strong exciton regulation of Raman scattering in monolayer  $\text{MoS}_2$ . *98*, 161405.

- (18) Profeta, M.; Mauri, F. Theory of resonant Raman scattering of tetrahedral amorphous carbon. *Physical Review B* **2001**, *63*, 245415.
- (19) Stock, G.; Domcke, W. Theory of resonance Raman scattering and fluorescence from strongly vibronically coupled excited states of polyatomic molecules. *The Journal of Chemical Physics* **1990**, *93*, 5496–5509.
- (20) Peticolas, W. L.; Rush, T. Ab initio calculations of the ultraviolet resonance Raman spectra of uracil. *Journal of Computational Chemistry* **1995**, *16*, 1261–1270.
- (21) Jarzecki, A. A.; Spiro, T. G. Ab initio computation of the UV resonance Raman intensity pattern of aqueous imidazole. *Journal of Raman Spectroscopy* **2001**, *32*, 599–605.
- (22) Neugebauer, J.; Hess, B. A. Resonance Raman spectra of uracil based on Kramers–Kronig relations using time-dependent density functional calculations and multireference perturbation theory. *The Journal of Chemical Physics* **2004**, *120*, 11564–11577.
- (23) Scholz, R.; Gisslén, L.; Schuster, B.-E.; Casu, M. B.; Chassé, T.; Heinemeyer, U.; Schreiber, F. Resonant Raman spectra of diindenoperylene thin films. *The Journal of Chemical Physics* **2011**, *134*, 014504.
- (24) Balakrishnan, G.; Jarzecki, A. A.; Wu, Q.; Kozłowski, P. M.; Wang, D.; Spiro, T. G. Mode Recognition in UV Resonance Raman Spectra of Imidazole: Histidine Monitoring in Proteins. *The Journal of Physical Chemistry B* **2012**, *116*, 9387–9395.
- (25) Warshel, A.; Dauber, P. Calculations of resonance Raman spectra of conjugated molecules. *The Journal of Chemical Physics* **1977**, *66*, 5477–5488.
- (26) Albrecht, A. C. “Forbidden” Character in Allowed Electronic Transitions. *The Journal of Chemical Physics* **1960**, *33*, 156–169.

- (27) Albrecht, A. C. On the Theory of Raman Intensities. *The Journal of Chemical Physics* **1961**, *34*, 1476–1484.
- (28) Albrecht, A. C.; Hutley, M. C. On the Dependence of Vibrational Raman Intensity on the Wavelength of Incident Light. *The Journal of Chemical Physics* **1971**, *55*, 4438–4443.
- (29) Myers Kelley, A. Resonance Raman and Resonance Hyper-Raman Intensities: Structure and Dynamics of Molecular Excited States in Solution. *The Journal of Physical Chemistry A* **2008**, *112*, 11975–11991.
- (30) Gong, Z.-Y.; Tian, G.; Duan, S.; Luo, Y. Significant Contributions of the Albrecht's A Term to Nonresonant Raman Scattering Processes. *Journal of Chemical Theory and Computation* **2015**, *11*, 5385–5390.
- (31) Guthmuller, J. Comparison of simplified sum-over-state expressions to calculate resonance Raman intensities including Franck-Condon and Herzberg-Teller effects. *The Journal of Chemical Physics* **2016**, *144*, 064106.
- (32) Eric J. Heller,; Yuan Yang,; Lucas Kocia,; Wei Chen,; Shiang Fang,; Mario Borunda,; Efthimios Kaxiras, Theory of Graphene Raman Scattering. *ACS Nano* **2016**, *10*, 2803–2818.
- (33) Duan, S.; Tian, G.; Luo, Y. Theory for Modeling of High Resolution Resonant and Nonresonant Raman Images. *Journal of Chemical Theory and Computation* **2016**, *12*, 4986–4995.
- (34) Hu, W.; Duan, S.; Luo, Y. Theoretical modeling of surface and tip-enhanced Raman spectroscopies. *WIREs Comput Mol Sci* **2017**, 1293.
- (35) Avila Ferrer, F. J.; Barone, V.; Cappelli, C.; Santoro, F. Duschinsky, Herzberg–Teller, and Multiple Electronic Resonance Interferential Effects in Resonance Raman Spectra

- and Excitation Profiles. The Case of Pyrene. *Journal of Chemical Theory and Computation* **2013**, *9*, 3597–3611.
- (36) Baiardi, A.; Bloino, J.; Barone, V. Accurate Simulation of Resonance-Raman Spectra of Flexible Molecules: An Internal Coordinates Approach. *Journal of Chemical Theory and Computation* **2015**, *11*, 3267–3280.
- (37) Heller, E. J.; Yang, Y.; Kocia, L. Raman Scattering in Carbon Nanosystems: Solving Polyacetylene. *ACS Central Science* **2015**, *1*, 40–49.
- (38) Kramers, H. A.; Heisenberg, W. Über die Streuung von Strahlung durch Atome. *Zeitschrift für Physik* **1925**, *31*, 681–708.
- (39) Dirac, P. a. M. The Quantum Theory of Dispersion. *Proceedings of the Royal Society of London A: Mathematical, Physical and Engineering Sciences* **1927**, *114*, 710–728.
- (40) Breit, G. Quantum Theory of Dispersion. *Reviews of Modern Physics* **1932**, *4*, 504–576.
- (41) Jensen, L.; Autschbach, J.; Schatz, G. C. Finite lifetime effects on the polarizability within time-dependent density-functional theory. *The Journal of Chemical Physics* **2005**, *122*, 224115.
- (42) Neese, F.; Petrenko, T.; Ganyushin, D.; Olbrich, G. Advanced aspects of ab initio theoretical optical spectroscopy of transition metal complexes: Multiplets, spin-orbit coupling and resonance Raman intensities. *Coordination Chemistry Reviews* **2007**, *251*, 288–327.
- (43) Lee, S. Placzek-type polarizability tensors for Raman and resonance Raman scattering. *The Journal of Chemical Physics* **1983**, *78*, 723–734.
- (44) Jensen, L.; Zhao, L. L.; Autschbach, J.; Schatz, G. C. Theory and method for calculating resonance Raman scattering from resonance polarizability derivatives. *The Journal of Chemical Physics* **2005**, *123*, 174110.

- (45) Montero, S. Anharmonic Raman intensities of overtones, combination and difference bands. *The Journal of Chemical Physics* **1982**, *77*, 23–29.
- (46) Hemert, M. C. V.; Blom, C. E. Ab initio calculations of Raman intensities; analysis of the bond polarizability approach and the atom dipole interaction model. *Molecular Physics* **1981**, *43*, 229–250.
- (47) András Stirling, Raman intensities from Kohn–Sham calculations. *The Journal of Chemical Physics* **1996**, *104*, 1254–1262.
- (48) Shinohara, H.; Yamakita, Y.; Ohno, K. Raman spectra of polycyclic aromatic hydrocarbons. Comparison of calculated Raman intensity distributions with observed spectra for naphthalene, anthracene, pyrene, and perylene. *Journal of Molecular Structure* **1998**, *442*, 221–234.
- (49) Jackson, K.; Pederson, M. R.; Porezag, D.; Hajnal, Z.; Frauenheim, T. Density-functional-based predictions of Raman and IR spectra for small Si clusters. *Physical Review B* **1997**, *55*, 2549–2555.
- (50) Umari, P.; Pasquarello, A. Infrared and Raman spectra of disordered materials from first principles. *Diamond and Related Materials* **2005**, *14*, 1255–1261.
- (51) Ferrari, A. C.; Robertson, J. Interpretation of Raman spectra of disordered and amorphous carbon. *Physical Review B* **2000**, *61*, 14095–14107.
- (52) Piscanec, S.; Mauri, F.; Ferrari, A. C.; Lazzeri, M.; Robertson, J. Ab initio resonant Raman spectra of diamond-like carbons. *Diamond and Related Materials* **2005**, *14*, 1078–1083.
- (53) Rousseau, D. L.; Williams, P. F. Resonance Raman scattering of light from a diatomic molecule. *The Journal of Chemical Physics* **1976**, *64*, 3519–3537.



- (54) Dierksen, M.; Grimme, S. Density functional calculations of the vibronic structure of electronic absorption spectra. *The Journal of Chemical Physics* **2004**, *120*, 3544–3554.
- (55) Moran, A. M.; Egolf, D. S.; Blanchard-Desce, M.; Kelley, A. M. Vibronic effects on solvent dependent linear and nonlinear optical properties of push-pull chromophores: Julolidinemalononitrile. *The Journal of Chemical Physics* **2002**, *116*, 2542–2555.
- (56) Jarzecki, A. A. Quantum-Mechanical Calculations of Resonance Raman Intensities: The Weighted-Gradient Approximation. *The Journal of Physical Chemistry A* **2009**, *113*, 2926–2934.
- (57) Wächtler, M.; Guthmuller, J.; González, L.; Dietzek, B. Analysis and characterization of coordination compounds by resonance Raman spectroscopy. *Coordination Chemistry Reviews* **2012**, *256*, 1479–1508.
- (58) Korenowski, G. M.; Ziegler, L. D.; Albrecht, A. C. Calculations of resonance Raman cross sections in forbidden electronic transitions: Scattering of the  $992\text{ cm}^{-1}$  mode in the  $1B_{2u}$  band of benzene. *The Journal of Chemical Physics* **1978**, *68*, 1248–1252.
- (59) Woodward, L. A.; Long, D. A. Relative intensities in the Raman spectra of some Group IV tetrahalides. *Transactions of the Faraday Society* **1949**, *45*, 1131–1141.
- (60) Mortensen, J. J.; Hansen, L. B.; Jacobsen, K. W. Real-space grid implementation of the projector augmented wave method. *Physical Review B* **2005**, *71*, 035109.
- (61) Enkovaara, J.; Rostgaard, C.; Mortensen, J. J.; Chen, J.; Dułak, M.; Ferrighi, L.; Gavnholt, J.; Glinsvad, C.; Haikola, V.; Hansen, H. A.; Kristoffersen, H. H.; Kuisma, M.; Larsen, A. H.; Lehtovaara, L.; Ljungberg, M.; Lopez-Acevedo, O.; Moses, P. G.; Ojanen, J.; Olsen, T.; Petzold, V.; Romero, N. A.; Stausholm-Møller, J.; Strange, M.; Tritsarlis, G. A.; Vanin, M.; Walter, M.; Hammer, B.; Häkkinen, H.; Madsen, G. K. H.; Nieminen, R. M.; Nørskov, J. K.; Puska, M.; Rantala, T. T.; Schiøtz, J.; Thygesen, K. S.; Jacobsen, K. W. Electronic structure calculations with GPAW: a real-space

- implementation of the projector augmented-wave method. *Journal of Physics: Condensed Matter* **2010**, *22*, 253202.
- (62) Blöchl, P. E. Projector augmented-wave method. *Physical Review B* **1994**, *50*, 17953–17979.
- (63) Perdew, J. P.; Burke, K.; Ernzerhof, M. Generalized Gradient Approximation Made Simple. *Physical Review Letters* **1996**, *77*, 3865–3868.
- (64) Larsen, A. H.; Mortensen, J. J.; Blomqvist, J.; Castelli, I. E.; Christensen, R.; Marciniak, D.; Friis, J.; Groves, M. N.; Hammer, B.; Hargus, C.; Hermes, E. D.; Jennings, P. C.; Jensen, P. B.; Kermode, J.; Kitchin, J. R.; Kolsbjerg, E. L.; Kubal, J.; Kristensen, K.; Laasbjerg, S.; Lysgaard, S.; Maronsson, J. B.; Maxson, T.; Olsen, T.; Pastewka, L.; Peterson, A.; Rostgaard, C.; Schiøtz, J.; Schütt, O.; Strange, M.; Thygesen, K. S.; Vegge, T.; Vilhelmsen, L.; Walter, M.; Zeng, Z.; Jacobsen, K. W. The atomic simulation environment—a Python library for working with atoms. *Journal of Physics: Condensed Matter* **2017**, *29*, 273002.
- (65) M.E. Casida,; M. Huix-Rotllant, Progress in Time-Dependent Density-Functional Theory | Annual Review of Physical Chemistry. *Annual Review of Physical Chemistry* **2012**, *63*, 287–323.
- (66) Walter, M.; Häkkinen, H.; Lehtovaara, L.; Puska, M.; Enkovaara, J.; Rostgaard, C.; Mortensen, J. J. Time-dependent density-functional theory in the projector augmented-wave method. *The Journal of Chemical Physics* **2008**, *128*, 244101.
- (67) Oklopcić, A.; Hirata, C. M.; Heng, K. Raman Scattering by Molecular Hydrogen and Nitrogen in Exoplanetary Atmospheres. *The Astrophysical Journal* **2016**, *832*, 30.
- (68) Wolniewicz, L.; Staszewska, G.  $1\Sigma_u^+ \rightarrow X1\Sigma_g^+$  transition moments for the hydrogen molecule. *Journal of Molecular Spectroscopy* **2003**, *217*, 181–185.

- (69) Fantz, U.; Wunderlich, D. Franck–Condon factors, transition probabilities, and radiative lifetimes for hydrogen molecules and their isotopomers. *Atomic Data and Nuclear Data Tables* **2006**, *92*, 853–973.
- (70) Jong, M. d.; Seijo, L.; Meijerink, A.; Rabouw, F. T. Resolving the ambiguity in the relation between Stokes shift and Huang–Rhys parameter. *Physical Chemistry Chemical Physics* **2015**, *17*, 16959–16969.
- (71) W. S. Benedict,; N. Gailar,; Earle K. Plyler, Rotation-Vibration Spectra of Deuterated Water Vapor. *The Journal of Chemical Physics* **1956**, *24*, 1139–1165.
- (72) Benny G. Johnson,; Peter M. W. Gill,; John A. Pople, The performance of a family of density functional methods. *The Journal of Chemical Physics* **1993**, *98*, 5612–5626.
- (73) Dimitrij Rappoport, *Berechnung von Raman-Intensitäten mit zeitabhängiger Dichtefunktionaltheorie*; Univ.-Verl. Karlsruhe: Karlsruhe, 2007.
- (74) Caillie, C. V.; Amos, R. D. Raman intensities using time dependent density functional theory. *Physical Chemistry Chemical Physics* **2000**, *2*, 2123–2129.
- (75) Richards, C. M.; Nielsen, J. R. Raman Spectrum of 1,3-Butadiene in the Gaseous and Liquid States\*. *JOSA* **1950**, *40*, 438–441.
- (76) Chadwick, R. R.; Zgierski, M. Z.; Hudson, B. S. Resonance Raman scattering of butadiene: Vibronic activity of a bu mode demonstrates the presence of a 1Ag symmetry excited electronic state at low energy. *The Journal of Chemical Physics* **1991**, *95*, 7204–7211.
- (77) Phillips, D. L.; Zgierski, M. Z.; Myers, A. B. Resonance Raman excitation profiles of 1,3-butadiene in vapor and solution phases. *The Journal of Physical Chemistry* **1993**, *97*, 1800–1809.

- (78) Krawczyk, R. P.; Malsch, K.; Hohlneicher, G.; Gillen, R. C.; Domcke, W. 1 Bu–2 1Ag conical intersection in trans-butadiene: ultrafast dynamics and optical spectra. *Chemical Physics Letters* **2000**, *320*, 535–541.
- (79) Peng, Q.; Yi, Y.; Shuai, Z.; Shao, J. Toward Quantitative Prediction of Molecular Fluorescence Quantum Efficiency: Role of Duschinsky Rotation. *Journal of the American Chemical Society* **2007**, *129*, 9333–9339.
- (80) Hemley, R. J.; Dawson, J. I.; Vaida, V. Franck–Condon analysis of the  $1^1A_g^- \rightarrow 1^1B_u^+$  transition of 1,3-butadiene from absorption and Raman intensities. *The Journal of Chemical Physics* **1983**, *78*, 2915–2927.
- (81) Hsu, C.-P.; Hirata, S.; Head-Gordon, M. Excitation Energies from Time-Dependent Density Functional Theory for Linear Polyene Oligomers: Butadiene to Decapentaene. *The Journal of Physical Chemistry A* **2001**, *105*, 451–458.
- (82) Hsu, C.-P.; Hirata, S.; Head-Gordon, M. Excitation Energies from Time-Dependent Density Functional Theory for Linear Polyene Oligomers: Butadiene to Decapentaene. *The Journal of Physical Chemistry A* **2001**, *105*, 451–458.
- (83) Stefan Grimme, *Reviews in Computational Chemistry, Volume 20*; John Wiley & Sons, Inc, 2004; Vol. 20; p 153.
- (84) Guo, M.; He, R.; Dai, Y.; Shen, W.; Li, M.; Zhu, C.; Lin, S. H. Franck-Condon simulation of vibrationally resolved optical spectra for zinc complexes of phthalocyanine and tetrabenzoporphyrin including the Duschinsky and Herzberg-Teller effects. *The Journal of Chemical Physics* **2012**, *136*, 144313.
- (85) Keil, T. H. Shapes of Impurity Absorption Bands in Solids. *Physical Review* **1965**, *140*, A601–A617.

- (86) Resta, R. Manifestations of Berry's phase in molecules and condensed matter. *Journal of Physics: Condensed Matter* **2000**, *12*, R107.
- (87) Min, S. K.; Abedi, A.; Kim, K. S.; Gross, E. Is the Molecular Berry Phase an Artifact of the Born-Oppenheimer Approximation? *Physical Review Letters* **2014**, *113*, 263004.
- (88) Baer, R. Born–Oppenheimer invariants along nuclear configuration paths. *The Journal of Chemical Physics* **2002**, *117*, 7405–7408.
- (89) Casida, M. E. Time-Dependent Density-Functional Theory for Molecules and Molecular Solids. *Journal of Molecular Structure: THEOCHEM* **2009**, *914*, 3–18.